Chapter 5

H ELECTRONIC DECAY TO PROTON DECAY DRIVING SUBSEQUENT NUCLEAR REACTIONS

It is shown *infra.* that in the limit of H electronic decay corresponding to hydrino transitions to higher p quantum numbers and lower energy states causes the corresponding proton to decay to gamma rays and the ~1GeV energy released drives subsequent nuclear reactions such as photoneutron production, fission, spallation, neutron capture and neutron capture/beta decay. H electronic decay may also drive a fusion reaction by a similar mechanism as muonic catalyzed fusion. Ordinarily, fusion reaction rates are extraordinarily small [47]. In fact, fusion is virtually impossible in the laboratory. A high relative kinetic energy corresponding to extraordinary temperatures of the participating nuclei must be sufficient to overcome their repulsive potential energy. The recent NIF experimental results confirm that so called "ignition" requires 250,000,000°C and a deuterium-tritium density of ten times that of lead to achieve about 0.2% fusion power over that input to the NIF lasers. In this case, the lasers consumed 500 trillion watts of power, 33 times the peak power of the entire world![1]

Cold fusion regarding hydrogen loading, excess hydrogen absorbed in a metal lattice to form relatively chemically unstable compound palladium hydride, to force nuclei together is not possible since the Coulombic energy barrier for deuterium is 0.1 MeV [47]. Whereas the vibrational energies within crystals are much less, about 0.01 eV. Coulombic screening is also not plausible based on the known crystalline structure of metal hydrides. Given the relationship between temperature and energy, 11,600 K/eV, the disparity in temperature in both cases is 1.16 X 10^7 versus 116 K, a factor of one hundred thousand. Moreover, proton-proton fusion is not possible under any condition as shown by 13 TeV proton-proton collisions at CERN wherein fusion have never been observed.

Albeit, it is still high-energy physics involving colliders, muonic catalyzed fusion may propagate at a high rate at more conventional plasma temperatures. Rather than directly using high temperature and density conditions, fusion occurs by a muonic catalyzed mechanism involving forming muons in a high-energy accelerator that transiently replace electrons in atoms and molecules (time scale of the muon half-life of 2.2 μs). In muon catalyzed fusion [48-49], the internuclear separation of muonic H_2 is reduced by a factor of 207 that of electron H_2 (the muon to electron mass ratio), and the fusion rate increases by about 80 orders of magnitude. A few hundred fusion events can occur per muon (vanishingly small compared to Avogadro's number of $6.022X10^{23}$). To be permissive of even this miniscule rate of fusion, the muonic molecules provide the same conditions as those at high energies. Correspondingly, the vibrational energies regarding the movement of the nuclei towards each other in an oscillating linear manner can be very large in the muonic hydrogen case, $E_{vib} \approx \nu 207X\ 0.517\ eV = \nu 107\ eV$ wherein ν is the vibrational quantum number. During the close approach of the vibrational compression phase, the nuclei can assume an orientation that allows the mutual electric fields to induce multipoles in the quarks and gluons to trigger a transition to a fusion product. The highest vibrational energy states such as the state $\nu = 9$ with $E_{vib} \approx \nu 107\ eV = 9X107\ eV = 963\ eV$ are at the bond dissociation limit. Given the extraordinary confinement time in a bound state, these muonic molecules have sufficiently large kinetic energy to overcome the Coulombic barrier for fusion of the heavy hydrogen isotopes of tritium with deuterium at just detectable rates.

Fusion in the Sun occurs due to extreme gravitational compression and thermal temperatures that provide sufficient confinement time, enormous reactant densities, and incredible e137nergies. But even here, the Sun considered as a fusion machine of 1.412 X10^{30} *liter* outputting $3.846X10^{26}\ W$ corresponds to a feeble $272\ \mu W / liter$. Fusion bombs (e.g. Tsar Bomba) require ignition by a fission bomb that produces power density on the order of $\frac{240X10^{15}\ J}{\left(10^{-3}\ s\right)\left(2.7X10^{7}\ liters\right)} = 8.8X10^{12}\ W / liter$, $3.2X10^{16}$ times the average power density of the Sun.[2]

Next, consider the feasibility of hydrino catalyzed fusion (HCF) based on a similar mechanism to that of muonic catalyzed fusion. Once a deuterium or tritium hydrino atom is formed by a catalyst, further catalytic transitions

[1] It is also remarkable that the NIF device cost $3.5B, and the fusion pellet cost $1M for a single shot that requires months to repeat. The product was less than one cents worth of radioactive thermal as an explosive shock wave.

[2] Arc current detonation of hydrated silver shots and other conductive solid fuels comprising a source of hydrogen and a source of HOH catalyst yielded power densities comparable to those of nuclear weapons [50-54].

$n=\frac{1}{2}\rightarrow\frac{1}{3}$, $\frac{1}{3}\rightarrow\frac{1}{4}$, $\frac{1}{4}\rightarrow\frac{1}{5}$, and so on may occur to a limited extent in competition with molecular hydrino formation that terminates this cascade. The hydrino atom radius can be reduced to $1/p$ that of the $n=1$ state atom. Analogous to muonic catalyzed fusion, the internuclear separation in the corresponding hydrino molecules is $1/p$ that of ordinary molecular hydrogen as given in the Nature of the Chemical Bond of Hydrogen-Type Molecules and Molecular Ions section (Eq. (11.204)). As the internuclear separation decreases due to high p states, fusion is more probable. As p becomes large, relativistic effects (e.g. relativistic electron mass and kinetic energy) become appreciable for the energy transferred from a hydrino atom and accepted by the catalyst that provides the corresponding energy hole. As in the nonrelativistic case, the energy transferred is the potential energy of the hydrogen-type atom H(1/p) that transitions to a lower energy state, divided by p^2, the total number of multipole modes of the state according to Eq. (5.45). Due to similar relativistic effects in hydrino atoms of similar p states, hydrino atoms may serve as the catalyst by disproportionation reactions such as ones given by Eqs. (5.62-5.80). Disproportionation reactions may propagate or cascade to very low hydrino energy states of corresponding very high p values. The corresponding hydrino molecules have vastly shorter internuclear distances (Eq. (11.204)) such that finite rates of nuclear reactions may occur in the case of heavy hydrogen isotopes, deuterium and tritium.

In the case that the electron spin-nuclear interaction is negligible, using Eq. (1.292), the relativistic potential energy of a hydrino atom $H\left(1/p\right)$ of a given state p is

$$V=\frac{Ze^2}{4\pi\varepsilon_0 r}=\frac{Z^2e^2}{4\pi\varepsilon_0 a_0\sqrt{1-(\alpha Z)^2}}=\frac{(\alpha p)^2 m_{e0}c^2}{\sqrt{1-(\alpha p)^2}} \tag{5.112}$$

wherein the radius given by Eq. (1.289) is

$$r=\frac{a_0}{p}\sqrt{1-(\alpha p)^2} \tag{5.113}$$

and Eqs. (28.8-28.9) were used. Thus, the energy hole according to Eqs. (5.112), (5.5), and (5.45) is

$$m=\frac{\alpha^2 m_{e0}c^2}{\sqrt{1-(\alpha p)^2}} \tag{5.114}$$

which in the low-speed limit is $m\cdot 27.2\ eV$ given by Eq. (5.5). Using Eq. (1.294) and Eqs. (5.6-5.9), the energy released from a hydrino state p during the transition involving an energy hole of quanta m is given by the difference in ionization energies between the initial and final energy states wherein the final p_f state is $p_f=p+m$:

$$\Delta E=m_{e0}c^2\left(\sqrt{1-\left(\alpha p\right)^2}-\sqrt{1-\left(\alpha\left(p+m\right)\right)^2}\right) \tag{5.115}$$

In the low-speed-limit the energy released is given by Eq. (5.9).

Consider the hydrino photon electric field given by Eq. (5.27) that superimposes and increases the proton field at the position of the electron and the mechanism of its creation given in the Energy Hole Concept section. For sufficient energy available in the central electric field of the binding positive center, the highest p quantum number possible is p=137 due to the limiting speed of light for the bound electron. Otherwise, the p quantum number may be lower. In the case of a proton as the binding center, all the energy in the electric field of the proton is converted to relativistic kinetic energy and binding energy before the p =137 state can be reached. For H(1/p), the minimum radius corresponds to the energy level at which the total energy in electric field of the nucleus has been released as ionization energy and relativistic kinetic energy, the sum of which is given by Eq. (5.112). This total energy is the potential energy of the electric field of a proton given by Eqs. (1.261) and (5.112) wherein the radius is the radius of the proton given by Eq. (37.1):

$$V=\frac{e^2}{4\pi\varepsilon_0 r}=\frac{e^2}{4\pi\varepsilon_0 1.30\ X\ 10^{-15}m}=1.77\ X\ 10^{-13}J\ =\ 1.11X10^6 eV \tag{5.116}$$

Then, the minimum radius and the maximum value of p is determined by equating Eq. (5.112) to Eq. (5.116):

$$\frac{(\alpha p)^2 m_{e0}c^2}{\sqrt{1-(\alpha p)^2}}=1.77\ X\ 10^{-13}J\ =\ 1.11X10^6 eV \tag{5.117}$$

The reiterative solution of Eq. (5.116) is p = 126 corresponding to a minimum radius of $1.651X10^{-13}$ m. Using Eq. (5.115), the energy for the cascade of a hydrogen atom to the final state of H(1/126) results in an energy release of 2×10^5 eV. This energy release process is the basis of a clean, non-nuclear power source that is autonomous of the grid and fuels infrastructure with a projected on-site electricity generation cost of $0.001/kWh, a factor of about 200 times less expensive than other power sources [59].

Next consider the consequences of a producing a hydrogen atom with the minimum radius of $1.651X10^{-13}$ m by driving the cascade of hydrino transition reactions to this state. The radius of a muonic hydrogen is given by the Bohr radius (Eq. (1.256)) with the mass of the electron replaced by the mass of the muon, $1.883X10^{-28}$ kg resulting in a radius of $2.560\ X10^{-13}$ m. Comparing the muon radius to the minimum hydrino radius demonstrates that in the limit, the hydrino atom H(1/126) is 1.55 times smaller than the muonic hydrogen atom such that the fusion rates should be comparable. Unlike inertial confinement

fusion and confined plasma fusion that require temperatures on the order of 10^8 K, muonic catalyzed fusion may occur at close to room temperature, so it was dubbed "cold fusion". However, muonic catalyzed fusion is not cold in the sense that long confinement times at very high vibrational energies are required to cause the close approach of the fusing nuclei against the nuclear coulombic repulsion [60]. The non-relativistic vibrational energies for molecular hydrino are given by Eq. (11.223) as $E_{vib} = p^2 0.517\ eV$, and the relativistic atomic radii are given by Eq. (5.113). A sufficiently high p can provide vibrational energies and close approach of nuclei of corresponding molecules sufficient for fusion to ensue. Considering the p^2 dependency of the vibrational energies of $H_2(1/p)$, and excitation of highest vibrational energy state at the bond dissociation limit (e.g. $v = 9$), the state $p = 15$ can achieve comparable vibrational energies as muonic molecules; yet, the $p = 15$ hydrino atomic radius (Eq. (5.113) and corresponding molecular hydrino internuclear distance are about 14 times greater than those of the muonic species. The p state that achieves comparable dimensions to those of muonic atoms and molecules is $p = 115$ (Eq. (5.113)) which has a corresponding nonrelativistic vibrational energy of 6840 eV. Only the lowest energy vibrational state would likely be populated with the energy from bond formation $p^2 4.478eV$ (Eq. 11.252)) since the temperature required to excite 7 keV vibrational modes is on the order of 10^8 K, compared to an ordinary plasma temperature of about 1000 K. Considering that the muon catalysis event occurs on the time scale of 0.5×10^{-12} [61], and the internuclear distance of hydrogen-isotopic molecular hydrino such $^2H_2(1/p)$ and $^3H_2(1/p)$ may be shorter than the corresponding muonic molecules, very high fusion rates may be achieved with a large population of high-p-state molecular hydrinos.

Hydrino Catalyzed Fusion (HCF) has utility to produce (i) neutrons (D + T and D + D fusion), and (ii) ^{3}He, tritium, and high energy protons (D + D fusion) which have industrial applications. Using heavy hydrogen, trace production of tritium by HCF may be competitive with atomic accelerators and hot fusion reactors. According to a study by Kovari [62], D-D tritium breeding might cost $2 billion per kilogram tritium produced. Tritium stockpiles are projected to be depleted near term wherein Savannah River's tritium facilities are the United States' only source of tritium, an essential component in nuclear weapons.

Consider the consequence of the formation of the state wherein p =127. In this case the central photon field may increase without sufficient energy to increase the relativistic kinetic energy of the electron required to maintain a stable non-radiative orbit. Specifically, the increased electric field due to the photon results in the corresponding central electric field force exceeding the centrifugal force. In this case, the electron may collapse onto the proton, and the proton may decay. The products of the widely believed pathway for proton decay are a positron and a neutral pion that further decays into two gamma rays. In the hydrino decay pathway, the hydrino electron annihilates the positron and emits two 511 keV photons. The ***total energy release of 930.8 MeV*** is that of the annihilation of H(1/126) which is the sum of the mass energy of the proton (931 MeV) and the electron (511 keV) minus the binding energy of H(1/126) (200.9 keV) given by Eq. (5.115). The reaction is given by:

$$\begin{array}{lccc} H(1/p) \rightarrow & e^+ + e^- + & \pi^0 & \\ & \downarrow & \downarrow & \\ & 2\gamma & 2\gamma & \end{array} \tag{5.118}$$

wherein e^+ is the positron, e^- is the electron, π^0 is the neutral pion, and γ is a gamma ray. Collision of the positron with the electron produces the characteristic 511 keV annihilation energy emission. 511 keV radiation is observed as a distinct peak in the cosmic gamma ray spectrum (Figure 5.4) wherein the origin is yet unknown [63-68].

Figure 5.4. Fit of the spectrum of the positron annihilation emission measured by SPI with narrow and broad Gaussian lines and an ortho-positronium continuum (Prantzos et al., 2010, ref. [67]).

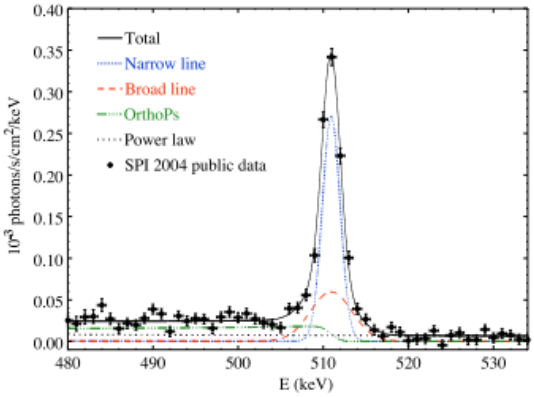

A forerunner explanation of the diffuse 511keV positron annihilation emission [63-68] with no point source [64] and a narrow line-width [67-68] is decaying dark matter [63-68] that is consistent with the ***hydrino as the identity of dark matter*** as given in the Composition of the Universe section and Refs.[9, 58] with ***H(1/p) decay (Eq. (5.118)) as the 511 keV source***. Further support of this assignment is that the neutral pion decay energy is also observed as a maximum intensity broad peak in the

cosmic gamma ray spectrum [69].

Specifically, the 511 keV gamma ray line intensity observed by the INTEGRAL/SPI experiment is consistent with the galactic bulge annihilation rate of ~ (1.5±0.1)×10^{43} low-energy positrons per second within ~ 1 kpc (3.26×10^3 light years) of the galactic center [63-64]. The prior inexplicable source of low-energy positrons from the Milky Way bulge is assigned to hydrino decay wherein hydrino is the identity of dark matter in agreement with many analyses indicating that dark matter decay is the most plausible assignment [63-68]. Consider the magnitude of mass of H atoms that undergo decay over the oscillatory cycle of the universe at the bulge rate corrected for the size of the galactic dark matter halo. The Milky Way is a barred spiral galaxy that is roughly 100,000 light years across and 1,000 light years thick. The Milky Way's dark matter halo is estimated to extend roughly 1,000,000 light-years in radius, meaning it is significantly larger than the visible bulge of the galaxy, which is around 5,000 light-years in radius [70]. The halo is thought to contain most of the galaxy's mass and is dominated by dark matter. The H(1/p) decay rate corrected for the volume of the halo relative to the sampled volume of the bulge is about 1.5×10^{50}. ***Multiplying dark matter-halo-corrected decay rate of 1.5×10^{50}/s times the oscillatory period of the universe of 9.83×10^{11} years (Eq. (32.149)) gives total mass of decayed hydrino atoms and corresponding protons of the Milky Way of 6.2×10^{42} kg compared to the total mass of the Milky Way galaxy of about 6×10^{42} kg [70].*** This estimate demonstrates that H(1/p) decay is a very prominent process in the evolution of the cosmos. The decay rate decreases with time in the expansion phase of the expansion-contraction cycle of the universe, but the measured rate is low since it assumes that the positron travels great distances before encountering an electron and annihilating whereas the positron annihilates with the electron of H(1/p) and does not travel. Further decay of proton mass/energy occurs through the mechanism of matter to energy conversion during fusion and other nuclear reactions culminating in the formation of black holes. Subsequently, when the mass density of a black hole reaches the threshold of the Planck mass density a gamma ray burst occurs contributing to the energy portion of the pathway of recycling of protons as given in Composition of the Universe section. Concerted H(1/p) decay may also give rise to gamma ray bursts consistent with the gamma ray spectrum recorded on a burst [71] showing a characteristic "π^0-decay bump" [69]. These are likely, the long duration, lower energy type gamma ray bursts.

In addition to 511 keV gamma ray emission, neutral pion π^0, gamma and X-ray, and neutron emission are observed from a broad array of astrophysical environments such as interstellar medium, supernova remnants (SNRs), molecular clouds, galaxy clusters, and other sources [69] as well as solar flares [72] and thunderstorms [73]. In the latter cases, the Italian Space Agency's AGILE observatory found that the energy spectrum of terrestrial gamma-ray flashes extends up to 100 MeV [74], and100 MeV gamma, 511 eV, as well as neutral pion decay radiation and neutrons were recorded on solar flare emission [72] wherein neutron emission was observed by 2.223 MeV emission due to the capture reaction with protons to form deuterium. Shane et al. [75] report on data from Fermi LAT of solar flare spectra showing the characteristic "π^0-decay bump" [69] and a cutoff of about 1 GeV. A proposed source of the Sun's gamma rays is decaying dark matter [76]. These signatures are characteristic of decay of hydrino atoms H(1/p) each comprising a proton and an electron in a high p state. The neutral pion π^0 emission has a distinct bell-type feature ("π^0-decay bump") between 100 MeV and a few GeV [69]. The energy of the mass to energy conversion of the proton's mass of 938.27 MeV and the electron's mass of 511 keV of a first hydrino may be transferred as kinetic energy or as a gamma ray to a proton such as that of a second hydrino in proximity, or alternatively to a proton of a hydrogen atom. The gamma ray incident a proton may give rise to neutron production. The neutron production reaction from hydrino decay is given by the photoneutron production reaction in hydrogen [77]:

$$\begin{array}{l} \gamma + p^+ \rightarrow n \; + \; \pi^+ \; + \quad \pi^0 \\ \qquad\qquad\quad \downarrow \qquad\quad \downarrow \\ \qquad\qquad\quad \mu^+ + \nu_\mu \qquad 2\gamma \\ \qquad\qquad\quad \downarrow \\ \qquad\quad e^+ + \; \nu_e \; + \; \bar{\nu}_\mu \\ \qquad\quad \downarrow e^- \\ \qquad\quad 2\gamma \end{array} \tag{5.119}$$

where p^+ is the proton, n is the neutron, π^+ is the positive pion, μ^+ is the positive muon, ν_e is the electron neutrino, ν_μ is the muon neutrino, and $\bar{\nu}_\mu$ is the muon antineutrino. The neutral pion decays to two gamma rays. The positive pion decays to a positive muon and a muon neutrino. The positive muon decays to a positron, an electron neutrino, and a muon antineutrino. The positron annihilates with an electron to produce two 511 keV gamma photons. Overall, photoneutron production from a proton additionally produces four gamma rays and three neutrinos, one of electron flavor and two of muon flavor. Another possible reaction is that the gamma ray energy of the decay of a first hydrino atom causes the production of an energetic neutron and an electron neutrino from a second hydrino atom:

$$\gamma \; + \; H\left(1/p\right) \; \rightarrow \; n \; + \; \nu_e \tag{5.120}$$

The pathway of Eq. (5.119) predicts 2 muon neutrinos to 1 electron neutrino which matches the results of solar neutrino experiments. Specifically, photoneutron production ***Eq. (5.119) predicts the relative number of electron to muon neutrinos being 1/3 and 2/3 of the total, respectively. The predicted electron and muon neutrino ratios match solar neutron observations by detectors such as the Homestake Solar Neutrino Experiment, GALLEX, SAGE, Sudbury Solar Neutrino***

Observatory, and Kamiokande and Super-Kamiokande detectors [78]. The results do not match the Standard Solar Model prediction of an electron neutrino intensity 3 times higher than observations with no muon neutrinos observed. The only direct evidence that fusion occurs in the Sun and stars is the solar neutrino data. However, the solar neutrino data indicate that the source of sunlight from the Sun is not only the p-p chain to form helium nuclei from protons by fusion. Rather the hydrino driven chain:

$$\textit{hydrino decay} - \textit{neutron production} - \textit{neutron capture} - \textit{beta decay} \tag{5.121}$$

contributes significantly. Proton-proton fusion has not been measured in the laboratory under any condition and may not occur in the Sun. The p-p chain may be initiated by protons undergoing neutron capture to form deuterium. Additionally, the neutron capture and beta decay reaction may repeat to higher atomic number elements as known in the formation of heavier nuclei than iron during supernova. The possibility that the p-p chain was not the only source of solar power was considered by Bahcall [78]. According to Bahcall, [78] the possibility of a revolutionary discovery of a new source of energy in the Sun based on a prior undiscovered process is an open question.

This neutron production reaction is more favorable for high-p-state H(1/p), and this reaction suppresses gamma emission from the primary hydrino decay reaction. The production of neutrons can be observed by the subsequent signature of neutron capture reactions. Neutron capture by protons to form deuterium produces a characteristic 2.223 MeV peak that is observed in cosmic gamma ray spectra [79-81] and spectra of solar flares [72] wherein the energy to drive the neutron-production reactions is assigned to proton decay of high-p-state hydrino atoms and molecules. Other nuclei of interstellar medium are capable of undergoing neutron capture resulting in isotope shifts and atomic number shifts. Abundances and depletions of other neutron-capture elements in addition to proton and deuterium nuclei have been observed in the interstellar medium consistent with a high neutron flux wherein the source of the neutrons is assigned to hydrino decay (Eq. (5.118)) [82-83].

The power from hydrino decay may be very high wherein the energy yield is equivalent to matter-antimatter annihilation. For example, the power of a solar flare can exceed that of one billion hydrogen bombs. Consider that the solar flare event is powered by the hydrino transition and decay reactions. These reactions are capable of positive feedback wherein the rates increase as the plasma temperature rises from reaction heating. Consider the limit of the highest p value for a hydrino state H(1/p). The energy release per hydrino atom decay in a so called "dark matter device" given by Eq. (5.118) is 930.8 MeV (1.49×10^{-10} J) corresponding to 89.8 TJ/mol, or 89,806 TJ/kg with no radioactive fuel or products involved and absent the requirement of a critical mass. As an atomic bomb comparison, the fission of one atom of uranium-235 locally releases 202.5 MeV (3.24×10^{-11} J) corresponding to 19.54 TJ/mol, or 83.14 TJ/kg with another 8.8 MeV that is lost as anti-neutrinos. As a chemical comparison, the energy released by detonation of 1 kg of TNT is 4.184 MJ. The hydrino decay reaction is thermonuclear in nature such that the reaction can go to completion. Any size material may be made to detonate by means such as the creation of an electrical arc or a shock wave in a material comprising at least one of high-p-state H(1/p) and H_2(1/p) initiated by a detonation of conventical explosive, explosive wire detonation, blasting caps, or use of other conventional detonators to create at least one of an arc, shock wave, and high thermal event. Given that the ***energy production of hydrino decay is 1080 times nuclear and 2.15×10^{10} times TNT, detonation of an exemplary energetic hydrino material comprising a 1g hydrino (H(1/p), p>>4) (less than the size of a sugar cube) can release 25 kilotons of explosive energy equivalent to twice that of early atomic bombs***. Serving as a fuel, 1 g of hydrino (H(1/p), p>>4) can provide enough energy to power over one million homes for a year. Additionally, hydrino decay can serve as a source of neutrons that can propagate transmutation by fission reactions such as fission of ^{235}U, ^{239}Pu, ^{7}Li, and ^{6}Li to form desired products such as energy, tritium, and neutrons. The fission energy release may further serve to drive thermonuclear fusion reactions for important applications such as radionuclide and isotope production or radioactive waste remediation, weapons, and power.

In the case of extraordinarily high p states approaching p = 126, bonding with inner shell electrons may result in fusion of higher atomic number elements than hydrogen. Such states wherein a high-p-state hydrino atom served as a "fat neutron" is supported by such a species formed by muonic atoms [84].

Another more favorable transmutation reaction pathway especially for heavy elements is by neutron capture. Specifically, a further application of neutron production by hydrino decay is transmutation by neutron capture followed by beta decay. In general, isotope transmutation occurs when nuclei absorb neutrons. This process may occur until an unstable isotope is formed and subsequently undergoes beta decay with an increase in atomic number, balance of proton to neutron ratio, and stability. Hydrino decay may serve as a neutron source. Transmutation by neutron capture or fission is valuable for several industrial applications such as production of elements and isotopes of elements with industrial applications such as radioisotopes for medical and labeling purposes and as nuclear fuel. Transmutation may also be useful for remediation of radioactive waste.

In addition to photoneutron production from high-energy gamma photons reacting with protons, high-energy gamma rays incident deuterium may cause photoneutron production [85] with a threshold of 2.223 MeV by the reaction:

$$\gamma + d^+ \rightarrow n + p^+ \tag{5.122}$$

where d^+ is the deuterium nucleus, p^+ is the proton, and n is the neutron. Several research laboratories report results consistent with the production of neutrons and neutron capture and well as transmutation reactions that are caused by neutron capture followed by beta decay from H and D reactants. The experiments like those reported by Mills et al. [86] involve creation of atomic hydrogen by aqueous electrolysis on a cathode comprising at least one of a metal and a co-deposited metal such as Ni, Pd, or Pt that is favorable to dissociate and absorb hydrogen wherein hydrino reactants comprising a source of H(D) and

HOH(DOD) catalyst are generated. Jones for example reports anomalous neutron emission from cathodes during aqueous electrolysis [87], and Smith et al. [88] report neutron emission from co-deposition cathodes during aqueous electrolysis. Palladium and platinum are examples of candidate elements wherein hydrino decay followed by neutron capture by the nucleus of a heavy element creates isotope ratios different from those of natural abundance wherein the product may decay by beta emission to form the element with the next higher atomic number. Palladium and platinum are known to undergo neutron capture followed by beta emission with silver [89-90] and gold [91] as the products, receptively. Gadly et al. [92] also report the emission of fast neutrons from Pd cathodes undergoing aqueous electrolysis recorded with a diamond detector, gas filled ^{3}He detectors after thermalization with high density polythene, as well as novel epoxy resin, and CR-39 detectors. Gadly et al. [92] further report observations of transmutation of the Pd to Ag consistent with the anticipated neutron capture-beta decay reaction. Consistent with neutron capture and neutron capture with beta decay Pala et al. [93] report the observation of Pt and Pd isotope shifts as well as transmutation of Pd to Ag and Pt to Au from isotope and elemental analysis (EDX, WDS, ICPMS, and ToF-SIMS) of a Pt cathode onto which Pd is co-deposited during aqueous electrolysis. High energy tracks in CR-39 detectors consistent with several neutron-induced carbon-12 nuclear splitting reactions were also reported indicating that the neutron energy was greater than the threshold of these reaction of 100 MeV [94]. Energetic neutron, particle, and gamma ray production recorded by CR-39 detectors on the co-deposition experiment were reported earlier by a group at SPAWAR [95-97] as well as other researchers [98].

Carbon does not readily undergo fission; it is considered too small and stable to split apart in a fission reaction, making it much more likely to participate in fusion instead, especially when considering its most abundant isotope, carbon-12. However, products of the over 1 GeV hydrino decay event are energetic neutrons. When high-energy neutrons collide with heavy nuclei, a reaction called spallation occurs, where the heavy nucleus is violently broken apart, emitting multiple smaller particles like protons, neutrons, alpha particles, and other lighter nuclei, effectively "spalling" or chipping away at the heavy nucleus; this process is often used to produce secondary beams of particles in particle accelerators. Spallation may also occur after a neutron is captured wherein the nucleus fragments into several parts. The process is important only at energies more than 100 MeV for the incident neutron, and the cross sections increase to energies as high as 400–500 MeV. Several neutrons may serve to carry increased energy to the spallation reaction whereby deexcitation gamma rays may be emitted [99]. Kumar et al. [100] also report spallation products in addition to isotope shifts and transmutation products during aqueous electrolysis.

H(1/p) of high p state may be produced by successive transitions of H(1/p) to lower-energy, higher p states catalyzed by other hydrino states once formed by HOH catalyst. This reaction requires long H(1/p) containment times, a source of activation energy, and a source of H(1/p) to serve as reactants and catalyst. Metal can serve as matrix as demonstrated by electrolysis at metal cathodes and by co-deposited metals on base metal cathodes [93, 95-98] wherein the HOH (DOD) catalyst and H (D) to form H(1/4) (D(1/4) are produced by aqueous electrolysis, and the applied electrical power may serve as the source of activation energy. In the case that the cathode comprises a water-reactive metal that reacts with the electrolyte to form atomic H on the cathode surface, the hydrino reaction may be enhanced by the production of H. For example, Kumar et al. [100] report superior transmutation results with a Kanthal cathode and a basic electrolyte wherein aluminum reacts with water in basic solution to evolve atomic H. The hydrino reaction may be promoted using hydrogen storage and dissociating materials, such as nickel, palladium, and platinum. Moreover, the hydrino reaction may be made more efficient by intermittent application of electrolysis current where in hydrogen created on the metal cathode surface, and the metal serves to dissociate as the metal absorbing releases hydrogen during the off phase of the intermittent cycle as shown by Mills et al. [86]. Gas chromatography of gas collected from the SunCell, a plasma based hydrino reaction system comping two molten tin injectors to maintain two intersecting molten metal streams, demonstrated the formation of high-p state H(1/p) [58] wherein supplied H_2 and trace O_2 supply the H and HOH catalyst, and at least one of the high temperature plasma, and a low voltage high current applied through the molten metal streams provided the activation energy. The high kinetic impact of ball milling also propagates chemical reactions [101]. EPR recorded on ball milled salts that provide a source of H and HOH catalyst as well as a matrix to trap hydrino demonstrated that high p states can be formed in this system as well [102]. A light source (e.g. high powered laser), a particle beam, or a high- or low-voltage high-current low-impedance electricity source may provide at least one of high power density irradiation, activation, arc plasma formation, and heating of solid (e.g. solid fuels reported by Mills et al. [8-12]), liquid (e.g. aqueous) , or gaseous hydrino reactants each comprising a source of H and a source of HOH to provide high reaction kinetics to form high-p-state H(/p) wherein at least one of the laser, particle beam, and high- or low-voltage high-current low-impedance electricity source provides the activation energy.

H(1/p) comprises an unpaired electron such that it is magnetic. Furthermore, molecular hydrino such as H_2(1/p) comprises a paired and an unpaired electron in a single molecular orbital (MO) with a current density function given by ½ (↑↑ + ↓↑) wherein the current density function of H_2(1/p) is given graphically by the sum of current density of Figure 11.2 plus ½ times the current of Figure 11.2 superimposed on its mirror image as given in the Parameters and Magnetic Energies Due to the Spin Magnetic Moment of H_2(1/4) section. The unpair MO electron gives rise to spin flip transitions observed by electron paramagnetic spectroscopy (EPR) and well as magnetism observed by magnetic susceptibility measurements [58, 103]. EPR was reported on a matrix material Ga(O)OH that had the rare ability to trap individual H_2(1/4) molecules in a gas-like state that allowed for the study of theoretically predicted fine structure in the EPR hydrino signature. Specifically, Hagen and Mills [102] reported the theoretically predicted g factor for the spin flip transition with the predicted extraordinary features of a series of multiplets due to fluxon linkage within a series of multiplets due to spin-orbital splitting between the diamagnetic paired and paramagnetic unpaired electron of the MO during the EPR transition.

As a sequel to the 2022 paper, Hagen and Mills [103] report a large down-field singlet signature and temperature dependencies recorded by EPR that confirm the theoretical prediction of the formation of molecular hydrino dimers $[H_2(1/p]]_2$ as an extension of ordinary hydrogen chemistry. H_2 is known to form dimers $[H_2]_2$ at cryogenic temperatures whereas $[H_2(1/p]]_2$ was shown to be stable at elevated temperatures. Moreover, at low temperatures, it was observed that $[H_2(1/4]]_2$ dimers side to side anti-paired to form tetramers that were not EPR active. As the temperature was raised the EPR singlet for the dimer reappeared at the predicted temperature. The results further show the production of $H_2(1/8)$ and $[H_2(1/8]]_2$ dimers indicating greater release of energy than production of $H_2(1/4)$.

The observation of the formation of a dimer between molecular hydrino $H_2(1/4)$ and H_2 ($[H_2\text{-}H_2(1/4)]$) and the temperature dependence of hydrogen release explains the massive amounts of hydrogen observed from salts containing molecular hydrino reported previously [58, 103]. These salts are not known to absorb any hydrogen and indicate a new very significant technology comprising the conversion of common salts to hydrogen storage materials which are of great industrial value. These results further indicate the entrapment of hydrino promotes the further entrapment by a magnetic attraction. Very high magnetic fields are possible as shown by Hagen and Mills [103]. The use of ferromagnetic material such as Ni electrolysis cathodes or the use of FeOOH in the case of ball milling [58] with the further application of an external magnetic field would further boost the entrapment of hydrino and promote the formation of high-p-state H(1/p). A further implication of the formation of H(1/p), $H_2(1/p)$, $[H_2(1/p]]_2$, $[H_2(1/p]]_4$,…, $[H_2(1/p]]_n$ and corresponding D and T species is that multiple neutrons may be formed via decay of H(1/p) or D(1/p) due to the increased favorability of hydrino species to undergo these reactions. Dineutrons [104] and possibly tetraneutrons [105] are known to exist.

Fusion is another possible reaction for hydrogen isotope nuclei that have acquired high kinetic energy from hydrino decay. This reaction is limited to light nuclei wherein the exemplary Coulonb barrier for proton-proton fusion is 1 MeV [106]. Miles et al. [107] report the production of helium-4 by nuclear fusion of deuterium during aqueous electrolysis. In this case, room temperature or so called "cold fusion" is possible via hydrino decay in addition to a hydrino-muonic mechanism, but as in the case of room temperature muonic catalyzed fusion the reaction mechanism is not cold.

Helium-4 can also be formed by hydrino-decay-produced neutrons causing fission the LiOH electrolyte used [108]. Specifically, ^{6}Li or ^{7}Li may undergo fission to ^{4}He and ^{3}H with additionally a neutron product in the case of ^{7}Li. Both fusion and hydrino decay are favorable for high-p-state H(1/p). Fusion and hydrino decay require a hydrino transition reaction cascade such as one propagated by disproportionation reactions to hydrino states of high p. The cascade is favored by (i) massive kinetics, (ii) hydrino and plasma confinement, and (iii) increasing duration of the hydrino reaction. One exemplary system to cause massive kinetics and hydrino and plasma confinement is detonation of hydrino reactant solid fuels under arc current conditions [54-58]. Hydrino confinement is achieved by using as a component of the reactor comprising at least one of (i) a source of an applied magnetic field and (ii) a cryogenic system, or a hydrino reactant mixture comprising at least one of (i) a solid material to absorb hydrino atoms such as a metal surface or bulk metal such as one that also absorbs H atoms (e.g. Ni, Ti, Pd, Pt, Nb, or Ta) [58], (ii) a magnetic material such as FeOOH or Fe_2O_3, that favors magnetic bonding of hydrinos [58], and (iii) an oxide such as a metal oxide such as GaOOH or Ga_2O_3 that binds hydrinos [58,102]. Mosier-Boss et al. [96] report a summary of the ***nuclear signatures of hydrino decay observed ubiquitously from astrophysical and terrestrial sources are also observed from aqueous electrolysis experiments at hydrogen absorbing cathodes. Specifically, the nuclear signatures of energy, neutrons, helium-4, tritium, gamma rays, X-rays, energetic particles, spallation products, isotope shifts, and transmutation of heavy elements were observed.*** The evidence for fusion [107] has an alternative fission explanation, and the fusion assignment is discounted due to the observation of the absence of the known branching ratios for helium and tritium products of the D-D fusion reaction [108], and tritium is also a separate product of photoneutron capture by deuterium.

REFERENCES

1. K. Akhtar, J. Scharer, R. L. Mills, Substantial Doppler broadening of atomic-hydrogen lines in DC and capacitively coupled RF plasmas**,** J. Phys. D, Applied Physics, Vol. 42, (2009), 42 135207 (2009) doi:10.1088/0022-3727/42/13/135207.
2. R. Mills, K. Akhtar, "Tests of Features of Field-Acceleration Models for the Extraordinary Selective H Balmer α Broadening in Certain Hydrogen Mixed Plasmas," Int. J. Hydrogen Energy, Vol. 34, (2009), pp. 6465-6477.
3. R. L. Mills, B. Dhandapani, K. Akhtar, "Excessive Balmer α Line Broadening of Water-Vapor Capacitively-Coupled RF Discharge Plasmas," Int. J. Hydrogen Energy, Vol. 33, (2008), pp. 802-815.
4. R. Mills, P. Ray, B. Dhandapani, "Evidence of an Energy Transfer Reaction Between Atomic Hydrogen and Argon II or Helium II as the Source of Excessively Hot H Atoms in RF Plasmas," Journal of Plasma Physics, (2006), Vol. 72, Issue 4, pp. 469-484.
5. J. Phillips, C-K Chen, K. Akhtar, B. Dhandapani, R. Mills, "Evidence of Catalytic Production of Hot Hydrogen in RF Generated Hydrogen/Argon Plasmas," International Journal of Hydrogen Energy, Vol. 32(14), (2007), 3010-3025.
6. R. L. Mills, P. C. Ray, R. M. Mayo, M. Nansteel, B. Dhandapani, J. Phillips, "Spectroscopic Study of Unique Line Broadening and Inversion in Low Pressure Microwave Generated Water Plasmas," J. Plasma Physics, Vol. 71, Part 6, (2005), pp. 877-888.
7. R. L. Mills, K. Akhtar, "Fast H in Hydrogen Mixed Gas Microwave Plasmas when an Atomic Hydrogen Supporting Surface Was Present," Int. J. Hydrogen Energy, 35 (2010), pp. 2546-2555, doi:10.1016/j.ijhydene.2009.12.148.
8. R. Mills, Y. Lu, R. Frazer, "Power Determination and Hydrino Product Characterization of Ultra-low Field Ignition of Hydrated Silver Shots", Chinese Journal of Physics, Vol. 56, (2018), pp. 1667-1717.

9. R. Mills, J. Lotoski, Y. Lu, "Mechanism of soft X-ray continuum radiation from low-energy pinch discharges of hydrogen and ultra-low field ignition of solid fuels", Plasma Science and Technology, Vol. 19, (2017), pp. 1-28.
10. R. Mills J. Lotoski, "H_2O-based solid fuel power source based on the catalysis of H by HOH catalyst", Int'l J. Hydrogen Energy, Vol. 40, (2015), 25-37.
11. R. Mills, J. Lotoski, J. Kong, G. Chu, J. He, J. Trevey, "High-Power-Density Catalyst Induced Hydrino Transition (CIHT) Electrochemical Cell." Int. J. Hydrogen Energy, 39 (2014), pp. 14512–14530 DOI: 10.1016/j.ijhydene.2014.06.153.
12. R. Mills, "Hydrino States of Hydrogen", https://brilliantlightpower.com/pdf/Hydrino_States_of_Hydrogen.pdf, submitted for publication.
13. R. L. Mills, R. Booker, Y. Lu, "Soft X-ray Continuum Radiation from Low-Energy Pinch Discharges of Hydrogen," J. Plasma Physics, Vol. 79, (2013), pp 489-507; doi:10.1017/S0022377812001109.
14. K. R. Lykke, K. K. Murray, W. C. Lineberger, "Threshold photodetachment of H^-," Phys. Rev. A, Vol. 43, No. 11, (1991), pp. 6104-6107.
15. D. R. Lide, *CRC Handbook of Chemistry and Physics*, 86th Edition, CRC Press, Taylor & Francis, Boca Raton, (2005-6), pp. 10-202 to 10-204.
16. K. K. Baldridge, J. S. Siegel, "Correlation of empirical δ(TMS) and absolute NMR chemical shifts predicted by ab initio computations," J. Phys. Chem. A, Vol. 103, (1999), pp. 4038-4042.
17. J. Mason, Editor, *Multinuclear NMR*, Plenum Press, New York, (1987), Chp. 3.
18. C. Suarez, E. J. Nicholas, M. R. Bowman, "Gas-phase dynamic NMR study of the internal rotation in N-trifluoroacetlypyrrolidine," J. Phys. Chem. A, Vol. 107, (2003), pp. 3024-3029.
19. C. Suarez, "Gas-phase NMR spectroscopy," The Chemical Educator, Vol. 3, No. 2, (1998).
20. H. Beutler, Z. Physical Chem., "Die dissoziationswarme des wasserstoffmolekuls H_2, aus einem neuen ultravioletten resonanzbandenzug bestimmt," Vol. 27B, (1934), pp. 287-302.
21. G. Herzberg, L. L. Howe, "The Lyman bands of molecular hydrogen," Can. J. Phys., Vol. 37, (1959), pp. 636-659.
22. P. W. Atkins, *Physical Chemistry*, Second Edition, W. H. Freeman, San Francisco, (1982), p. 589.
23. N. V. Sidgwick, *The Chemical Elements and Their Compounds*, Volume I, Oxford, Clarendon Press, (1950), p.1
24. A. Beiser, *Concepts of Modern Physics*, Fourth Edition, McGraw-Hill Book Company, New York, (1978), pp. 153-155.
25. M. D. Lamb, *Luminescence Spectroscopy*, Academic Press, London, (1978), p. 68.
26. P. Kurunczi, H. Shah, and K. Becker, "Excimer formation in high-pressure microhollow cathode discharge plasmas in helium initiated by low-energy electron collisions," Int. J. Mass Spectrosc., Vol. 205, (2001), pp. 277-283.
27. P. F. Kurunczi, K. H. Becker, "Microhollow Cathode Discharge Plasma: Novel Source of Monochromatic Vacuum Ultraviolet Radiation," Proc. Hakone VII, Int. Symp. High Pressure, Low Temperature Plasma Chemistry, Greifswald, Germany, Sept. 10 - 13, (2000), Vol. 2, p. 491.
28. P. Kurunczi, H. Shah, and K. Becker, "Hydrogen Lyman-α and Lyman-β emissions from high-pressure microhollow cathode discharges in $Ne-H_2$ mixtures," J. Phys. B: At. Mol. Opt. Phys., Vol. 32, (1999), L651-L658.
29. J. Wieser, D. E. Murnick, A. Ulrich, H. A Higgins, A. Liddle, W. L. Brown, "Vacuum ultraviolet rare gas excimer light source," Rev. Sci. Instrum., Vol. 68, No. 3, (1997), pp. 1360-1364.
30. A. Ulrich, J. Wieser, D. E. Murnick, "Excimer Formation Using Low Energy Electron Beam Excitation," Second International Conference on Atomic and Molecular Pulsed Lasers, Proceedings of SPIE, Vol. 3403, (1998), pp. 300-307.
31. D. R. Lide, *CRC Handbook of Chemistry and Physics*, 86th Edition, CRC Press, Taylor & Francis, Boca Raton, (2005-6), pp. 9-54 to 9-59.
32. R. Mills, "Spectroscopic Identification of a Novel Catalytic Reaction of Atomic Hydrogen and the Hydride Ion Product," Int. J. Hydrogen Energy, Vol. 26, No. 10, (2001), pp. 1041-1058.
33. B. J. Thompson, *Handbook of Nonlinear Optics*, Marcel Dekker, Inc., New York, (1996), pp. 497-548.
34. Y. R Shen, *The Principles of Nonlinear Optics*, John Wiley & Sons, New York, (1984), pp. 203-210.
35. B. de Beauvoir, F. Nez, L. Julien, B. Cagnac, F. Biraben, D. Touahri, L. Hilico, O. Acef, A. Clairon, and J. J. Zondy, Physical Review Letters, Vol. 78, No. 3, (1997), pp. 440-443.
36. E. Bulbul, M. Markevitch, A. Foster, R. K. Smith, M. Loewenstein, S. W. Randall, "Detection of an unidentified emission line in the stacked X-Ray spectrum of galaxy clusters," The Astrophysical Journal, Volume 789, Number 1, (2014).
37. A. Boyarsky, O. Ruchayskiy, D. Iakubovskyi, J. Franse, "An unidentified line in X-ray spectra of the Andromeda galaxy and Perseus galaxy cluster," (2014),arXiv:1402.4119 [astro-ph.CO].
38. Nico Cappelluti, Esra Bulbul, Adam Foster, Priyamvada Natarajan, Megan C. Urry, Mark W. Bautz, Francesca Civano, Eric Miller, Randall K. Smith, "Searching for the 3.5 keV Line in the Deep Fields with Chandra: The 10 ms Observations," The Astrophysical Journal, Vol. 854 (2), (2018), p. 179 DOI: 10.3847/1538-4357/aaaa68.
39. F. A. Cotton, "Chemical applications of Group Theory," 2nd Edition, Wiley Interscience, (1963), pp. 280-283.
40. F. Wilkinson, "Intramolecular Electronic Energy Transfer Between Organic Molecules," *Luminescence in Chemistry*, Edited by E. J. Bowen, D. Van Nostrand Co. Ltd., London, (1968), Chapter 8, pp. 154-182.
41. H. Morawetz, Science, 240, (1988), pp. 172-176.
42. O. Schnepp, Levy, M., J. Am. Chem. Soc., 84, (1962), pp. 172-177.
43. F. Wilkinson, *Luminescence in Chemistry*, Edited by E. J. Bowen, D. Van Nostrand Co. Ltd., London, (1968), pp. 155-182.
44. Th. Förster, *Comparative Effects of Radiation*, Report of a Conference held at the University of Puerto Rico, San Juan,

February 15-19, (1960), sponsored by the National Academy of Sciences; National Research Council, Edited by Milton Burton, J. S. Kirby-Smith, and John L. Magee, John Wiley & Sons, Inc., New York pp. 300-325.
45. F. Bueche, *Introduction to Physics for Scientists and Engineers*, McGraw-Hill, (1975), pp. 352-353.
46. J. D. Jackson, *Classical Electrodynamics*, Second Edition, John Wiley & Sons, New York, (1975), pp. 739-747.
47. J. D. Jackson, *Classical Electrodynamics*, Second Edition, John Wiley & Sons, New York, (1975), pp. 758-760.
48. F. J. Bueche, *Introduction to Physics for Scientists and Engineers*, McGraw-Hill Book Company, New York, (1986), pp. 261-265.
49. I. Levine, *Physical Chemistry*, McGraw-Hill Book Company, New York, (1978), pp. 420-421.
50. F. J. Bueche, *Introduction to Physics for Scientists and Engineers*, McGraw-Hill Book Company, New York, (1986), pp. 261-265.
51. http://en.wikipedia.org/wiki/Nuclear_fusion.
52. L. I. Ponomarev, "Muon catalyzed fusion," Contemporary Physics, Vol. 31, No. 4, (1990), pp. 219-245.
53. J. Zmeskal, P. Kammel, A. Scrinzi, W. H. Breunlich, M. Cargnelli, J. Marton, N. Nagele, J. Werner, W. Bertl, and C. Petitjean, "Muon-catalyzed dd fusion between 25 and 150 K: experiment," Phys. Rev. A, Vol. 42, (1990), pp. 1165-1177.
54. R. Mills, Y. Lu, R. Frazer, "Power Determination and Hydrino Product Characterization of Ultra-low Field Ignition of Hydrated Silver Shots", Chinese Journal of Physics, Vol. 56, (2018), pp. 1667-1717.
55. R. Mills J. Lotoski, "H_2O-based solid fuel power source based on the catalysis of H by HOH catalyst", Int'l J. Hydrogen Energy, Vol. 40, (2015), 25-37.
56. https://brilliantlightpower.com/pdf/Spectroscopy_Nansteel_Report_040219.pdf.
57. https://www.brilliantlightpower.com/wp-content/uploads/pdf/Free-Air-TNT-Analysis.pdf.
58. R. Mills, "Hydrino States of Hydrogen", https://brilliantlightpower.com/pdf/Hydrino_States_of_Hydrogen.pdf, submitted for publication.
59. https://brilliantlightpower.com/.
60. T. Yamashita, Y. Kino, K. Okutsu, et al, "Roles of resonant muonic molecule in new kinetics model and muon catalyzed fusion in compressed gas", Sci Rep 12, 6393 (2022). https://doi.org/10.1038/s41598-022-09487-0.
61. J. D. Jackson, "Catalysis of Nuclear Reactions between hydrogen isotopes by μ−-Mesons". Physical Review. (1957), 106 (2): 330. Bibcode:1957PhRv..106..330J. doi:10.1103/PhysRev.106.330.
62. https://www.science.org/content/article/fusion-power-may-run-fuel-even-gets-started#:~:text=According%20to%20Kovari's%20study%2C%20D%2DD,%242%20billion%20per%20kilogram%20produced.
63. A. C. Vincent, P. Martin, J. M. Cline, "Interacting dark matter contribution to the Galactic 511 keV gamma ray emission: constraining the morphology with INTEGRAL/SPI observations", https://arxiv.org/pdf/1201.0997.
64. G. De Cesare, "Searching for the 511 keV annihilation line from galactic compact objects with the IBIS gamma ray telescope", A&A 531, A56 (2011) DOI: 10.1051/0004-6361/201116516, https://www.aanda.org/articles/aa/pdf/2011/07/aa16516-11.pdf.
65. J. Knodlseder, et al., "The all-sky distribution of 511 keV electron-positron annihilation emission", Astronomy & Astrophysics manuscript no. 2063, November 7, 2018, https://arxiv.org/pdf/astro-ph/0506026.
66. J. Knodlseder, et al., "The all-sky distribution of 511 keV electron-positron annihilation emission", astro-ph/0506026, Masaki Mori, ICRR Group Internal Seminar, June 20, 2005,https://www.icrr.u-tokyo.ac.jp/~morim/Presentations/INTEGRAL511keV.pdf.
67. N. Prantzos, C. Boehm, A. M. Bykov, et al., "The 511 keV emission from positron annihilation in the Galaxy", (2010), https://arxiv.org/abs/1009.4620.
68. N. Prantzos, C. Boehm, A. M. Bykov, et al., "The 511 keV emission from positron annihilation in the Galaxy", Reviews of Modern Physics, Vol. 83, July (2011), pp. 1001–1056.
69. R. Yang, E. Kafexhiu1, F. Aharonian, "Exploring the shape of the γ-ray spectrum around the "π^0-bump", A&A, Volume 615, July (2018), A108, https://doi.org/10.1051/0004-6361/201730908, https://www.aanda.org/articles/aa/pdf/2018/07/aa30908-17.pdf.
70. https://en.wikipedia.org/wiki/Milky_Way.
71. National Aeronautics and Space Administration, Goddard Space Flight Center, Fermi Gamma-ray Space Telescope, "Overview of GRB spectral analysis", https://fermi.gsfc.nasa.gov/ssc/data/analysis/documentation/Cicerone/Cicerone_GRBs/Overview_GRB_Spec_Anal.html.
72. R. Ramaty, R. J. Murphy, C. D. Dermer, "On the origin of the pion-decay radiation in the 1982 June 3 solar flare", The Astrophysical Journal, 316:L41-L44,1987 May 1. https://articles.adsabs.harvard.edu/cgi-bin/nph-iarticle_query?1987ApJ...316L..41R&defaultprint=YES&filetype=.pdf.
73. J. R. Dwyer, D. M. Smith, et al., "Positron clouds within thunderstorms", Journal of Plasma Physics, Volume 81 , Issue 4 , August (2015), 475810405, DOI: https://doi.org/10.1017/S0022377815000549.
74. F. Fuschino, M. Marisaldi, "AGILE and TGFs Latest results & activities", 11th AGILE Science workshop, "Gamma-rays and Galactic Cosmic Rays", May 16-17, 2013, ASI Headquarters, Via del Politecnico, Rome.
75. G. H. Share, R. J. Murphy, et al., "Characteristics of sustained >100 MeV γ ray emission associated with solar flares", February 28, (2022), https://arxiv.org/pdf/1711.01511.

76. N. Wolchover, “The Sun Is Stranger Than Astrophysicists Imagined”, Quanta Magazine, May 1, 2019, https://www.quantamagazine.org/gamma-ray-data-reveal-surprises-about-the-sun-20190501/.
77. Costa, S., Ferroni, S., Gracco, V.G. et al., “Photoneutron production from the proton at high energy”, Nuovo Cimento A (1965-1970) Vol. 45, (1966), pp. 696–705, https://doi.org/10.1007/BF02721135.
78. J. N. Bahcall, “Solving the mystery of the missing neutrinos”, **The Nobel Prize**, https://www.nobelprize.org/prizes/themes/solving-the-mystery-of-the-missing-neutrinos/#:~:text=Combining%20the%20SNO%20and%20the%20Super%2DKamiokande%20measurements%2C,as%20the%20number%20of%20just%20electron%20neutrinos.&text=Only%20the%20water%20detectors%20(Kamiokande%2C%20Super%2DKamiokande%2C%20and,of%20the%20solar%20neutrinos%20that%20are%20observed.
79. R. Diehl, “Cosmic Gamma-Ray Spectroscopy”, July 17, 2013, https://arxiv.org/pdf/1307.4198.
80. A. M. Ritchey , S. R. Federman, and D. L. Lambert, “Abundances and Depletions of Neutron-capture Elements in the Interstellar Medium”, The Astrophysical Journal Supplement Series, 236:36 (40pp), 2018 June, DOI 10.3847/1538-4365/aab71e, https://iopscience.iop.org/article/10.3847/1538-4365/aab71e/pdf.
81. D. J. Mullan, J. L. Linsky, “Nonprimordial deuterium in interstellar medium”, The Astrophysical Journal, Vol. 511, No. 1, (1999), pp. 502-512, DOI 10.1086/306650, https://iopscience.iop.org/article/10.1086/306650/pdf.
82. A. M. Ritchey , S. R. Federman, and D. L. Lambert, “Abundances and Depletions of Neutron-capture Elements in the Interstellar Medium”, The Astrophysical Journal Supplement Series, 236:36 (40pp), 2018 June, DOI 10.3847/1538-4365/aab71e, https://iopscience.iop.org/article/10.3847/1538-4365/aab71e/pdf.
83. D. J. Mullan, J. L. Linsky, “Nonprimordial deuterium in interstellar medium”, The Astrophysical Journal, Vol. 511, No. 1, (1999), pp. 502-512, DOI 10.1086/306650, https://iopscience.iop.org/article/10.1086/306650/pdf.
84. E. A. G. Armour, “Muon catalyzed fusion”, Symposium on Atomic & Molecular Physics, pp. 211-226; https://ntrs.nasa.gov/api/citations/20080040752/downloads/20080040752.pdf.
85. D. A. Fynan, Y. Seo, G. Kim, S. Barros, M. Jin Kim, “Photoneutron production in heavy water reactor fuel lattice from accelerator-driven bremsstrahlung”, Annals of Nuclear Energy, Vol. 155, June, 1, (2021), p. 108141 https://doi.org/10.1016/j.anucene.2021.108141.
86. R. L. Mills and S. Kneizys, “Excess heat by the electrolysis of aqueous potassium carbonate and the implications for cold fusion”, Fusion Technol. Vol. 20, (1991), p. 6.
87. S. E. Jones, “Anomalous neutron emission from metal-deuterium system”, (1990), (RAL--90-022). Davies, J.D. (Ed.). United Kingdom, https://inis.iaea.org/Search/searchsinglerecord.aspx?recordsFor=SingleRecord&RN=21081049
88. P. J. Smith, R. C. Hendricks, B. M. Steinetz, “Electrolytic co-deposition neutron production evaluation,” (NASA report No. E-19924), (2021).
89. J. D. Kraus, J. M. Cork, “Radioactive Isotopes of Palladium and Silver from Palladium”, Phys. Rev. 52, 15 October, (1937), p. 763, DOI: https://doi.org/10.1103/PhysRev.52.763.
90. https://en.wikipedia.org/wiki/Isotopes_of_palladium.
91. N. Petersen, “Measuring Neutron Absorption Cross Sections of Natural Platinum via Neutron Activation Analysis”, A thesis submitted to Oregon State University, Department of Physics, Corvallis, Oregon, June 11, 2012; https://ir.library.oregonstate.edu/downloads/4m90dx05b
92. Gadly, T., Phapale, S., Gamre, S. et al. Experimental and theoretical validation for transmutation of palladium at electrochemical interfaces. Sci Rep 14, 21270 (2024). https://doi.org/10.1038/s41598-024-70597-y.
93. R. G. S. Pala, K. P. Rajeev, A. Kumar, R. Nehra, “Low Energy Nuclear Reactions via Electrolysis”, 2024 ANS Annual Conference, June 16–19, 2024, https://dev.ans.org/meetings/ac2024/session/view-2545; https://www.ans.org/meetings/ac2024/session/view-2545/#paper_7627
94. E. L. Alpen, **Radiation Biophysics**, Second Edition (1998), Chapter 5 - Energy Transfer Processes, pp. 78-103.
95. P. Mosler-Boss, S. Szpak, F. E. Gordan, L. P. G. Forsley, “Triple tracks in CR-39 as the result of Pd-D co-deposition: evidence of energetic neutrons”, Naturwissenschaften, (2009) Jan;96(1):135-42. doi: 10.1007/s00114-008-0449-x.
96. P. A. Mosier-Boss, L. P. Forsley, “Chapter 2 - Review of Pd/D co-deposition”, Cold Fusion Advances in Condensed Matter Nuclear Science, (2022), pp. 17-36, https://www.sciencedirect.com/science/article/abs/pii/B9780128159446000026.
97. P. A. Mosier-Boss, S. Szpak, F. E. Gordon, L. P. G. Forsley, “Use of CR-39 in Pd/D codeposition experiments,” European Physical Journal Applied Physics, Vol. 40, (2007), pp. 293–303.
98. C. Gotzmer, L. F. DeChiaro, K. Conley, M. Litz, M. Millett, J. Ewing, L. P. Forsley, et al. "Li–Pd–Rh- D2O electrochemistry experiments at elevated voltage," APL Energy 1, no. 3, (2023); https://doi.org/10.1063/5.0153487.
99. S. Leray, “Nuclear reaction at high energy,” CEA/Saclay, DAPNIA/SPhN, Gif-surYvette Cedex, France, Workshop on Nuclear data for Science and Technology: Accelerator Driven Waste Incineration, Trieste, 10-21 September 2001, LNS0212005,https://www.osti.gov/etdeweb/servlets/purl/20909666.
100. A. Kumar, P. Jain, K. P. Rajeev, R. G. Pala, "Upper Bound in the Fusion Products and Transmutation Enhancement in Alloys", Journal of Condensed Matter Nuclear Science 36 (1), 327-335 (20202), https://jcmns.scholasticahq.com/article/72607-upper-bound-in-the-fusion-products-and-transmutation-enhancement-in-alloys.
101. T. Markmaitree, R. Ren, L. L. Shaw, “Enhancement of lithium amide to lithium imide transition via mechanical activation”, J. Phys. Chem. B., Vol. 110, No. 41, pp. 20710-20718.
102. Wilfred R. Hagen, Randell L. Mills, “Electron Paramagnetic Resonance Proof for the Existence of Molecular Hydrino”,

Vol. 47, No. 56, (2022), pp. 23751-23761; https://www.sciencedirect.com/science/article/pii/S0360319922022406.
103. Wilfred R. Hagen, Randell L. Mills, "General EPR pattern from molecular hydrino produced in various reactors", (2024), submitted; https://brilliantlightpower.com//pdf/General_EPR_pattern_from_molecular_hydrino_produced_in_various_reactors.pdf.
104. S. B. Borzakov, "Singlet Deuteron, Dineutron and Neutral Nuclei", FLNP JINR, Dubna, Russia, (Julu, (2023), DOI: 10.48550/arXiv.2307.12719.
105. A. Deltuva, R. Lazauskas, "Tetraneutron resonance in the presence of a dineutron", Phys. Rev. C 100, 044002 – Published 30 October, 2019, https://doi.org/10.1103/PhysRevC.100.044002.
106. Briefing on Low-Energy Nuclear Reactions (LENR) Research, A scientific survey of the international literature in response to the FY16, NDAA (report on HR4909, 4 May 2016), Office of the ASD(R&E) I Research, https://www.esd.whs.mil/Portals/54/Documents/FOID/Reading%20Room/Science_and_Technology/16-F-1333_%20DOC_02_LENR_Briefing.pdf.
107. M. H. Miles, P. Hagelstein, "Consistency of helium production with the excess power in the palladium-D2O electrochemical system", Journal of Electroanalytical Chemistry, Vol. 977, (2025), pp. 118786, DOI:10.1016/j.jelechem.2024.118786.
108. Fusion Physics, Edited by M. Kikuchi, K. Lackner, M. Q. Tran, IAEA International Atomic Energy Agency, p. 22, https://nucleus.iaea.org/sites/fusionportal/SiteCollectionDocuments/Fusion%20Book.pdf.